Sensors & Actuators: B. Chemical 309 (2020) 127712

Contents lists available at ScienceDirect

Sensors and Actuators B: Chemical

journal homepage: www.elsevier.com/locate/snb

Metalloporphyrins into mesoporous photonic crystals: towards molecularly-tuned photonic sensing devices

Rolando M. Caraballo[1], Diego Onna[1], Nicolás López Abdala, Galo J.A.A. Soler Illia, Mariana Hamer*

Instituto de Nanosistemas, Universidad Nacional de San Martín-CONICET, Av. 25 de Mayo 1021, San Martín, Buenos Aires, Argentina

ARTICLE INFO

Keywords:
Porphyrin
Photonic crystal
Hybrid material
Optical sensor
Detection
Amines

ABSTRACT

Metalloporphyrins are molecules capable of optically sensing targets due to their specific reactivity, and mesoporous photonic architectures can act as environment-responsive materials. In this work, we used a metalloporphyrin, Mn^{III} meso-tetra(N-methyl-4-pyridyl) porphyrin (MP), to add a recognition functionality to a mesoporous oxide photonic crystal (MOPC) in order to develop a versatile and portable sensing device for volatile amines exploiting both the open MOPC pore network and the high affinity of volatile amino analytes to the MP. The hybrid material MP@MOPC was prepared by immersion of the MOPC, synthesized from mesoporous silica and titania layers, in an MP solution. The system was characterized by UV–vis absorption and FTIR spectroscopies, and SEM microscopy. Sensing of small molecules was tested using ethylenediamine (EDA) as a volatile amine model, showing an absorbance increase in the MOPC spectral window with promising analytical parameters. The hybrid material presents enhanced sensing capabilities compared to the MP or MOPC components alone. A prototype device was built, aiming for a future design of simple, low-cost equipment, with a light emitting diode and a light-dependent resistor, which includes the MP@MOPC sensor.

1. Introduction

Detection of volatile organic amines is a field of growing interest. These molecules can be encountered in diverse areas, such as environmental and industrial monitoring [1–3], sanitary control of food [4] and medical diagnosis [5,6]. In particular, volatile amines are related to the degradation of meat and fish, indicating their quality or freshness state [7–9]. Detection, quantification and monitoring of volatile amines are thus a major concern for food and packaging industry and considered a relevant problem to solve through analytical chemistry methods.

In the last decades, the development of novel and simple analytical devices to detect and quantify target amines, with high sensitivity and resolution over very short times, has gained great attention [7–11]. One of the most promising strategies is in the optical sensing, which is easy to implement due to state-of-the-art technologies and can attain high sensitivity, selectivity, stability and real time detection [12]. Chemical binding of the analyte to specific colored reagents is a very common approach, when in presence of the amine some optical property (such as absorbance or emission spectra) is modified [13]. Among the vast variety of options, metalloporphyrins are excellent molecules for sensing specific targets [14,15]. These molecules have a highly tunable reactivity that can be modified through the metal center or the peripheral functional groups, as well as high chemical and thermal stability. From an optical point of view, they have unique electronic absorption characteristics with sharp and intense bands in the visible region arising from an extensively delocalized π-electron distribution [16]. Furthermore, metalloporphyrins have been used in constructing optical sensing membranes for detection of volatile organic compounds (VOC) because of their open coordination sites for axial ligation and their intense coloration [16–18]. However, metalloporphyrins absorbance spectral shifts observed upon VOC binding are relatively small, less than 30 nm, making it necessary to use a spectrophotometer for transducing the analyte concentration [19].

Photonic crystals (PC) are periodic optical structures that possess a photonic band-gap and can therefore be used to restrict the propagation of light [20]. This permits to control how light behaves inside these materials through their design, producing effects that are not possible with conventional optics. PC have been used for label-free detection of analytes, as the adsorption of small molecules produces changes in the

* Corresponding author.
E-mail address: mhamer@unsam.edu.ar (M. Hamer).
[1] These authors participated equally in the development of this work.

https://doi.org/10.1016/j.snb.2020.127712
Received 14 October 2019; Received in revised form 13 December 2019; Accepted 13 January 2020
Available online 01 February 2020
0925-4005/ © 2020 Elsevier B.V. All rights reserved.

refractive index and a spectral shift in the spectrum [21]. This shift can be detected with a spectrophotometric device or even with the naked eye. One common possible design implies one-dimensional PC made up of multilayered structures [22,23], which can be constructed using mesoporous oxides, leading to a Mesoporous Oxide Photonic Crystal (MOPC), and is responsive to vapors [24,25]. These materials have high surface area/volume ratios, which increases the interaction between the analyte and the active sensing component and, therefore, the sensitivity of the device, posing an interesting advantage compared to other sensing mechanisms [26]. In addition, the introduction of a tailored optical defect within the band gap permits to advantageously use a narrow wavelength interval for analytical purposes [27].

Furthermore, this feature can be combined by adding a molecular selective building block able to give a specific signal towards an analyte. The possibility of modifying the pore surfaces with organic or organometallic functional groups permits to confer selectivity through specific interactions towards analytes with different chemical structures [24].

In this work, we combine a specific metalloporphyrin, manganese (III) 5,10,15,20-[meso-tetrakis(N-methylpyridyl) porphyrin] (MP), embedded into an MOPC resonator, in order to develop a versatile and portable sensing device for volatile amines. The MOPC structure was pre-designed as an optical resonator, which provides a narrow transmission window within the forbidden frequency gap at a specific spectral region corresponding to the Soret band of the MP. In this way, the photonic structure presents a sensitive spectral change upon binding of ethylenediamine (EDA), which is used as a volatile amine model. This hybrid material was characterized and its sensing capabilities were explored for the components themselves and as part of a simple device. It was shown to be a sensitive optical probe for volatile amines detection.

2. Materials and methods

2.1. Materials and reagents

Manganese (III) 5,10,15,20-[meso-tetrakis(N-methylpyridyl) porphyrin] (MP) was purchased from Frontier Scientific. Titanium (IV) isopropoxide (TTIP), tetraethyl orthosilicate (TEOS), Pluronics F127, ethylenediamine (EDA), acetylacetone (AcAc) and concentrated HCl were purchased from Sigma-Aldrich Argentina. Ethanol was purchased from Biopack. Water was deionized and filtered using a Millipore water purification system (18 MΩ).

2.2. Photonic crystals (PC) synthesis

MOPC containing a mesoporous defect layer (i.e., leading to a mesoporous resonator) were prepared by successive dip-coating/consolidation cycles on glass and silicon substrates at 20 % relative humidity and at different withdrawal speeds, depending on the layer thickness required. Pluronics F127 was used as mesopore templating agent, while TTIP and TEOS were used as inorganic precursors for titania and silica thin films respectively. For titania films, a solution containing TTIP:EtOH:H_2O:AcAc:HCl:F127 with a molar ratio of 1:40:20:1:1:0.005 was prepared. In the case of silica, a first pre-hydrolysis step is performed by refluxing 1 h a water-ethanol solution, with $[H_2O]/[Si] = 1$, $[EtOH]/[Si] = 5$ and $[HCl]/[Si] = 10^{-5}$. After this step, reagents were added to the pre-hydrolyzed solution to obtain a final molar ratio of TEOS:EtOH:H_2O:HCl:F127 of 1:40:18:0.008:0.005. This solution was then aged at room temperature for 72 h under agitation and kept at -20 °C to prevent further ageing. After the deposition of each layer, the films were left at 50 % relative humidity for 30 min and submitted to a stabilizing thermal treatment consisting of three successive 30 min steps at 60 °C, 130 °C, and 200 °C to consolidate the inorganic matrix before template removal. This treatment is very important, because it allows the deposition of new layers without dissolution or degradation of the preceding ones. Finally, the multilayered structure is left at 350 °C for 2 h under air atmosphere to eliminate the templating agents.

2.3. Metalloporphyrin - photonic crystal systems (MP@MOPC)

The modification of the MOPC surface with the organic component was done by immersion in a 30 μM solution in water of MP for 48 h [28]. After adsorption, the MP@MOPC film was rinsed with deionized water and dried in a vacuum oven at 40 °C for 6 h.

2.4. Characterization

UV-Vis absorption spectra were recorded with an HP8453 diode array spectrophotometer in forward transmission mode using normal incidence geometry.

FTIR spectroscopy was performed on a Nicolet iN10 MX FTIR spectrometer in reflectance mode. All spectra were obtained as an average of 32 scans, at a 4.0 cm^{-1} resolution, in a range between 4000 and 650 cm^{-1}. Infrared data were processed using EZ-Omnic software.

Field Emission Scanning Electron Microscopy (FE-SEM) images were taken on a SEM Zeiss Supra 40 equipped with a field emission gun.

2.5. Photonic crystals modelling

Electromagnetic simulations were done with Lumerical FDTD Solutions environment. 2D Finite-Difference Time-Domain simulations were performed using a plane wave source and rectangular mesh elements, with Bloch boundary conditions on the X axis and Perfectly Matched Layer on the Y axis. Each layer was allowed to differ randomly ± 5 nm from its designed thickness due to experimental uncertainty, and the best matching structure was chosen. Table S1 shows the parameters used for the optical simulation.

2.6. Sensing assays

The sensitivity of MP towards EDA was demonstrated through UV–Vis absorption spectroscopy. Firstly, the experiments were performed with MP in solution, with increasing concentrations of EDA. Then, sensing assays in gas phase were done exposing an MP@MOPC film to increasing volume fractions of EDA vapors. These absorbance analytical studies were performed adding successive aliquots (1 mL) of EDA vapor inside the gas chamber. The procedure was repeated three times for each film and the average value was expressed with the corresponding error bars. In order to compare the sensing performance of the MP@MOPC films, three different batches were prepared and analytically tested, and the same behavior was observed. Nonetheless, variability in the preparation of the MOPC multilayer could limit the reproducibility.

Finally, both approaches were used to build a prototype for a future low-cost module for detection with a blue LED ($\lambda_{MAX} = 448$ nm) as the light source and a Light-Dependent Resistor (LDR) MLG5516 as the detector. The circuit diagram and LED characteristics are shown at Figure S1.

3. Results and discussion

3.1. Preparation of the mesoporous photonic architectures

Alternated mesoporous thin films of SiO_2 and TiO_2 were deposited on a glass substrate, which led to a one-dimensional periodic structure on the z-axis, generating an MOPC. This MOPC possessed a photonic bandgap which hindered the propagation of selected wavelengths as they passed through the material. Titania and silica were selected as the component layers because their refractive index contrast is optimal in order to obtain a significant transmission dip with few layers [29–32].

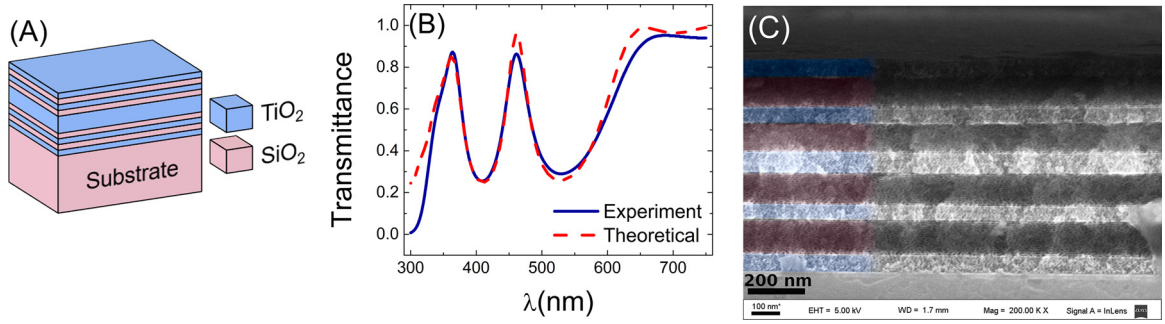

Fig. 1. (A) Scheme of the designed MOPC, SiO_2 layers are indicated in pink and TiO_2 layers in blue. (B) Theoretical (dashed line) and experimental (solid line) transmittance spectra of MOPC. The parameters used for the calculation are presented in Table S1. (C) FE-SEM image of the MOPC, SiO_2 layers are indicated with pink and TiO_2 layers with blue (For interpretation of the references to colour in this figure legend, the reader is referred to the web version of this article).

An optical defect was introduced in the form of a thicker mesoporous layer, as schematized in Fig. 1A, which disrupted the periodicity and allowed the transmission of a narrow frequency range within this photonic bandgap. The MOPC architecture behaves indeed as a resonator, which was designed selecting the range to propagate light around 460 nm, where the MP spectra presents an absorption band that changes with high sensitivity in the presence of amines.

A theoretical model of the material composed of two Bragg mirrors composed of 2x[SiO_2 (90 nm; $V_{Porosity}$ = 40 %) - TiO_2 (65 nm; $V_{Porosity}$ = 35 %)] thickness and an inserted TiO_2 layer of 130 nm thickness and 35 % porosity was proposed and the transmission spectrum (Fig. 1B, dashed line) was calculated taking into account the refractive indexes of mesoporous SiO_2 and TiO_2, according to a Bruggeman effective medium model [24]. This design was further used to prepare the MOPC with the desired layers thickness and porosity, leading to a material with the transmittance spectrum presented in Fig. 1B (solid line). Theoretical and experimental spectra are in excellent agreement, demonstrating that one can successfully move from the design to the synthesis of the MOPC. In addition, the electromagnetic field distribution by using FDTD simulation analysis was also obtained and is depicted in Figure S2.

Fig. 1C shows a high-resolution FE-SEM image of the MOPC. The cross-sectional image demonstrates a constant thickness for SiO_2 and TiO_2 layers, observed as darker and lighter layers in the image, respectively, because of the difference in the electronic density for each material. Additionally, the pore network of the MOPC, necessary to host the metalloporphyrin molecules, was clearly observed in both oxides [24]. Ellipsometric porosimetry was used to characterize the monolayers films porosity. This feature is confirmed as vapors can condensate within the porous thin films, shown in the isotherms of Figure S3.

3.2. Preparation of MP immobilized MOPC (MP@MOPC)

The inclusion of the metalloporphyrin inside the mesopores of the MOPC is summarized in the schematic representation shown in Fig. 2A. When the MOPC film is immersed in an MP solution, molecules pervade inside the pores and are adsorbed on their wall surface. After this process, when the film is observed on a tilted position, a slight orange coloration could be observed with the naked eye. Furthermore, the colour change was clearly appreciable on the powder produced by scrapping the films (Fig. 2B).

On the other hand, spectroscopic evidence of the inclusion of the MP within the mesopore system was obtained from UV–vis absorption spectra of the films (Fig. 3A). The absorbance increase around 460 nm can be attributed to MP incorporation. Figure S4 shows the resulting spectra using an MOPC as blank; MP@MOPC UV–vis absorption spectrum exhibits an intense absorption corresponding to the MP Soret band at λ = 462 nm. It is worth noting that the band position inside the pores remained the same as in solution, reflecting that the MP is bound through electrostatic interactions and not by coordination to Mn(III) nor self-assembly aggregation on the surface [15]. In fact, electrostatic interactions are expected to play a major role, since MP has a net positive charge, and TiO_2 and SiO_2 surfaces are negatively charged at near neutral pH [33,34].

UV-Vis spectroscopy was useful, not only to characterize the hybrid material, but also to estimate the amount of MP adsorbed in the film. Based on the absorbance of the Soret band of MP@MOPC and using the molar absorptivity of MP in solution ($\varepsilon^{463} = 1.29 \times 10^5\ M^{-1}.\ cm^{-1}$ [35]), the calculation of MP adsorbed inside the pores is estimated at 1.05×10^{-5} mol. cm^{-3} as a result, implying around 1.6 molecules per pore (see SI). Although MP are large molecules and the diffusion inside the pore network is limited due to the high tortuosity of the mesoporous material [26,36], it was observed that relatively large molecules, such as dihexadecyl phosphate, permeated in all layers in a multilayer mesoporous film [37].

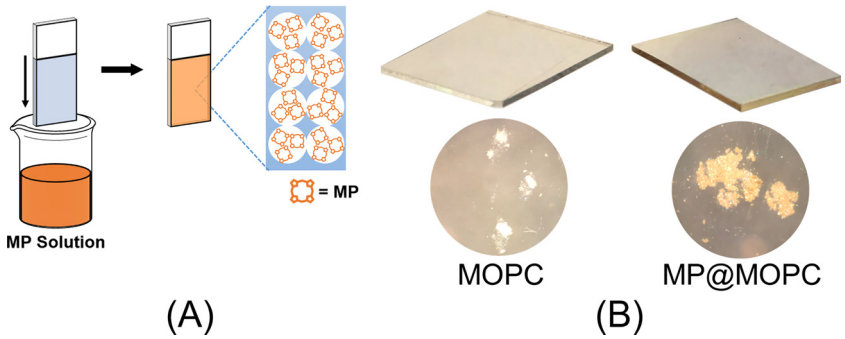

Fig. 2. (A) Schematic representation of MP immobilization on a mesoporous MOPC; (B) pictures of MOPC and MP@MOPC films, with a magnification of the scrapped material.

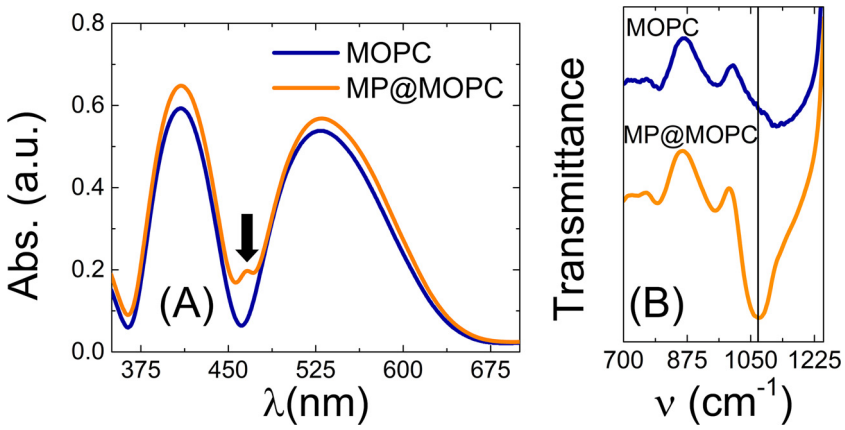

Fig. 3. (A) UV–vis absorption spectra of MOPC and MP@MOPC; (B) FTIR spectra of MOPC and MP@MOPC.

The presence of MP was also confirmed through by FTIR spectroscopy, as shown in Fig. 3B. It is worth mentioning that the fraction of MP adsorbed was relatively small, and so was the intensity of the signals. In the mid-frequency range (700–1250 cm^{-1}), the MP@MOPC film presents a band at 1070 cm^{-1} that corresponds to aromatic C–H bending and NC═ aza stretching [38].

It is worth noting that there is no alteration of the MOPC surface after the addition of MP, as no residues or pore clogging were observed in the FE-SEM images (Figure S5).

3.3. Quantitative analysis

The employed metalloporphyrin presents the ability to bind a variety of small molecules, such as NO, NO_2 and amines, among others [14]. Thus, MP is the receptor for the selective detection of analyte in the hybrid material. Binding of Lewis base analytes generally occurs through coordination to the metalloporphyrin's metallic center (Figure S6). In this work, EDA is used as a model to study the response of MP to volatile amines produced upon meat degradation, such as putrescine and cadaverine [7,8].

In order to assess the response of MP towards EDA binding, solution studies were first performed. UV–vis absorption spectra were measured when MP in solution (8 μM) was exposed to different concentrations of EDA and are shown in Fig. 4A. Black arrows indicate the main spectral changes observed, which become more evident in the difference absorption spectra presented in Fig. 4B. The absorbance at 443 nm exhibited an increment, while a decrease was observed at 462 nm. This occurs because aliphatic amines such as EDA act as sigma-donor ligands, coordinating to the metallic center and increasing the electronic density over it. Then, through metal-centered orbitals oriented towards the porphyrin structure, electron density on the aromatic rings also increases. As a result, the electronic transitions corresponding to the Soret band shift to higher energies compared to uncoordinated MP, modifying its UV–vis absorption spectra [39,40].

Fig. 4C shows the absorbance difference at 443 nm, where the observed response is higher. The absorbance increases until a saturation is reached after [EDA] = 130 ppm, corresponding to a 1:275 MP:EDA ratio. The reciprocal difference absorbance at 443 nm shows a linear behavior with respect to 1/[EDA] (Figure S7). From this plot, known as Benesi-Hildebrand [41], an associative constant for the coordination reaction was determined. The resulting value of K = 2544 M^{-1} is high compared to other porphyrins [42], showing a high affinity of MP for EDA.

In order to study the interaction of volatile amines with immobilized MP, we subsequently exposed MP@MOPC to increasing vapor pressures of EDA. The UV–vis absorption spectra were measured for each EDA concentration (Fig. 5A) and the absorption difference spectra were plotted (Fig. 5B). Minor differences were observed in the spectral band positions of MP@MOPC compared to spectra in solution because of the background of the holder and chamber used to perform the measurements (Figure S8). As expected, the coordination of EDA to MP@MOPC produces a blue shift of the Soret band, which is more discernible in the difference spectra. The higher sensitivity is achieved at 452 nm, and the absorbance difference at this wavelength is plotted against EDA concentration (Fig. 5C). A linear behavior is observed (m = 0.00216 ppm^{-1}, r^2 = 0.9958), meaning that the hybrid material is capable of detecting the volatile amine with a the linear range between 20 and 160 ppm. The detection limit was 15 ppm and the quantification limit of 46 ppm. The comparison of the analytical performance of MP@MOPC with related systems yields promising results, since the sensitivity and linear range are comparable to the merit figures of the latest generation amine sensors based on porphyrins absorbance spectra (Table S2). It is worth noting that the detection limit is one of the lowest found in the literature for similar molecular systems and almost an immediate response (≈ 10 s) was observed. In addition, this device is capable of sensing with only 1.52 μg of MP on a 1 cm^2 glass slide and it is easily prepared, leading to a truly cost-effective optical detection system.

The refractive index of MP@MOPC changed upon partial filling of the pores, shifting the position of both the photonic defect transmission window to lower energies. Thus, both changes in MP absorbance (due to EDA coordination) and on refractive index (because of pore filling with EDA and environmental humidity) occurred together in MP@MOPC. However, the variation in the absorbance spectrum for MP@MOPC upon EDA binding is significantly higher than the one observed

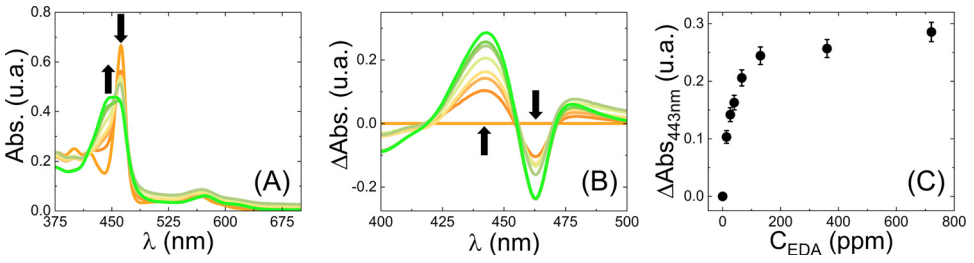

Fig. 4. (A) Absorbance spectra of MP (8 μM) with varying EDA amounts in the solution phase (13 − 720 ppm). The arrows indicate the changes in absorbance with increasing in EDA concentrations. (B) Difference absorbance spectra of MP in solution, in the presence of different EDA concentrations. (C) Absorbance difference at 443 nm for MP in the presence of different EDA concentrations.

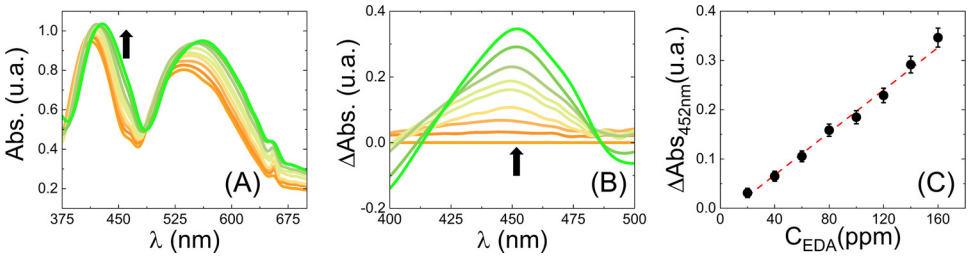

Fig. 5. (A) Absorbance spectra of MP@MOPC with varying EDA amounts in the gas phase (20 − 160 ppm). The arrows indicate the changes in absorbance with an increase in EDA concentration. (B) Difference absorbance spectra of MP@MOPC in the presence of different EDA concentrations. (C) Absorbance difference at 452 nm for MP@MOPC in the presence of different EDA concentrations.

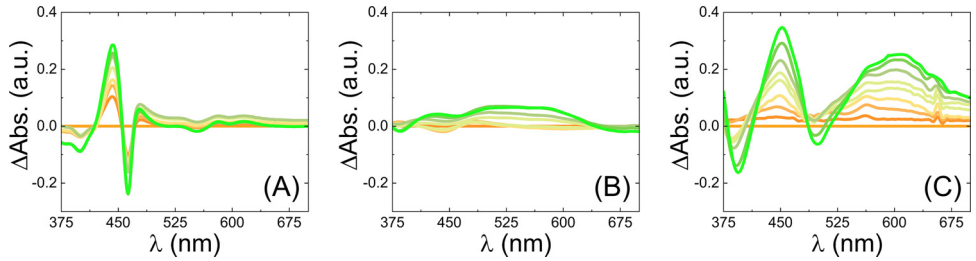

Fig. 6. Difference absorbance spectra of (A) MP in solution (8.0 μM); (B) MOPC; and (C) MP@MOPC in the presence of varying EDA concentrations.

in the cases of exposing the MP or the MOPC alone to the amine (Fig. 6). This fact proves that MP@MOPC presents a synergistic effect of the photonic architecture and the sensing molecule compared to the isolated components.

Sensing by MOPC is usually achieved using the optical shift ($\Delta\lambda/\lambda$) arising from changes in the refractive index [43,44]. Therefore, the transmittance optical shifts for MP@MOPC towards different EDA concentrations were calculated, using the same principle with both the two maxima and the two minima (Figure S9). The average optical shifts of MP@MOPC for each EDA concentration showed a linear behavior ($m = 0.0002\ ppm^{-1}$; $r^2 = 0.975$), with a detection limit of 26 ppm and a quantification limit of 87 ppm. Although this shift can be used for sensing, its detection and quantification limits are higher than the absorbance at 452 nm and, also, it is harder to implement on cheap sensing devices.

In the case of MOPC based sensors, spectral changes due to condensation are reversible. As for the hybrid system MP@MOPC, spectral changes did not reverse as easily to its initial state when purged using soft conditions, as the former case to did. This may occur because a stronger coordination is involved. However, this feature could be attractive in the development of a fresh-not fresh scenario, resulting in food quality assurance.

By means of these results, we obtained a distinctive optochemical sensor for the detection of volatile amines, based on a coordination reaction with MP within a highly porous MOPC, that lead to a shift on the porphyrin absorption spectra. The response was reproducible, and MP@MOPC sensors, when kept in dark and dry conditions, were found to be stable for more than twelve months after their fabrication.

3.4. MP@MOPC: towards a sensing device

In order to demonstrate the versatility of MP@MOPC for the development of future low-cost equipment, a prototype device was built with a blue LED as the light source ($\lambda_{MAX} = 448$ nm) and a light-dependent resistor (LDR MLG5516) as the detector (Fig. 7A). This wavelength was selected because it overlaps with the region of greater sensitivity of MP@MOPC, as shown in the previous section.

To assess the dependence of the device response on EDA, the MP@MOPC sensor was exposed to increasing vapor concentrations. A behavior similar to MP@MOPC in the previous section was observed. The measured resistance grew along increasing EDA partial pressure, until saturation was observed (Fig. 7B). The reciprocal resistance presents a linear behavior with respect to $1/C_{EDA}$ (Fig. 7C), becoming the most appropriate signal response for the sensing device ($m = 3\ ppm\ K\Omega^{-1}$; $r^2 = 0.961$). It is worth mentioning that the signal here is integrated under the source excitation spectrum, and thus response is subject to a higher error. For the device, a very fast response (≈ 10 s) was also observed.

These results prove that this simple and portable prototype is appropriate to be used for on-site quantification of volatile amines. Furthermore, a second channel can be implemented in the future, comprising the spectral changes around 600 nm. This improvement on the device might lead not only to quantify the analyte, but to differentiate between different volatile amines.

4. Conclusions

In this work we designed a hybrid material combining a metalloporphyrin (MP) and a mesoporous oxide photonic crystal architecture (MOPC). MP introduces the molecular recognition capability, while the MOPC component acts as an optical filter and as the hosting architecture for the binding reaction of the analytes. This combination can be used to detect volatile amines with competitive merit figures, compared to state-of-the-art optical sensors. Even more, this hybrid material presents a synergic behavior between the components that enhance the sensing effect. The pores of the material were available for the adsorption of the gaseous species and allowed the transduction of the binding process inside of them, with the coordination of EDA to the MP metal center being the main driving force of the phenomenon.

Although in this work we used EDA as a model to study the response of MP to volatile amines, our work demonstrates the applicability of functionalized MOPC as simple optically based chemical sensors. These results allow us to envisage the potential of this platform, since the selectivity and sensitivity of the device can be in principle further modulated by three main modifications: (i) the metallic ion center of the metalloporphyrin, which can be used to tune the affinity; (ii) the layer thickness and refractive indices, selecting the optical filter range, (iii) the mesopore size and their functionalization, which acts as molecular building blocks towards selectivity. In addition, all the MOPC materials and processing presented here are compatible with commercial electronic and optics platforms, permitting to scale-up these systems for portable applications. Last, but not least, these MOPC are robust, stable along time, and yield reproducible signals. Therefore, this design is very promising and it can be used to foresee a simple, versatile, device with high stability, specificity and low cost that facilitates early and accurate determination of volatile amines, thus reducing

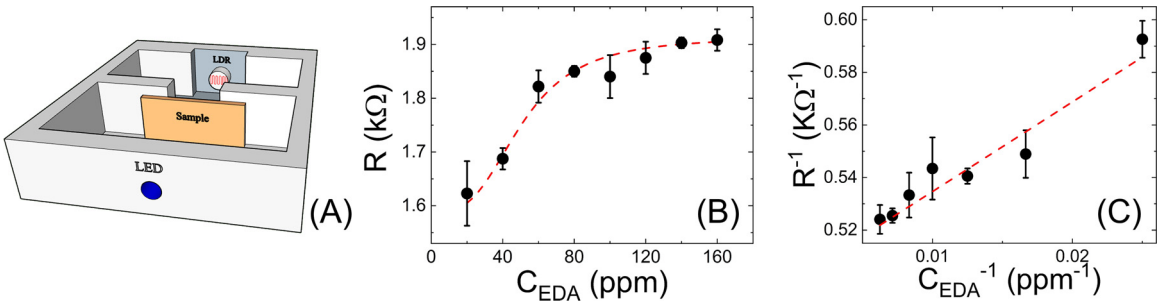

Fig. 7. (A) Scheme of the developed portable device. (B) Change in the signal (resistance) with increasing EDA vapor concentration. (C) R^{-1} vs C_{EDA}^{-1} plot.

potential health hazards.

Implementation of the hybrid material in a simple sensing device is shown through a prototype assembled with low cost, readily accessible materials. This is a starting point for future developments on widely accessible, point-of-care sensing devices.

Declaration of Competing Interest

The authors declare that they have no known competing financial interests or personal relationships that could have appeared to influence the work reported in this paper.

Acknowledgements

This work was financially supported by ANPCyT (PICT 2015-3526, 2016-0982 and 2017-4651) and UNSAM. N.L.A., D.O. and R.M.C. thank CONICET for the fellowship grant. G.J.A.A.S.I. and M.H. are members of CONICET. Authors thank Daniel Kimura for giving access to Lumerical software and Mark P. Kreuzer for the critical review and proofreading of the manuscript.

Appendix A. Supplementary data

Supplementary material related to this article can be found, in the online version, at doi:https://doi.org/10.1016/j.snb.2020.127712.

Parameters used for the optical simulation in Lumerical Software. Circuit diagram of the sensing device. Emission spectrum of the blue LED. Electromagnetic and magnetic field distribution at different wavelength and position calculated by FDTD simulation. Isotherms of water adsorption measured by Environmental Ellipsometric Porosimetry for monolayers of SiO_2 and TiO_2. UV–vis absorption spectra of MP in solution and MP@MPPC with PC as blank. Scanning electron microscope images of PC and MP@MOPC. Schematic representation of the reaction between MP and EDA. Benesi-Hildebrand plot for the absorbance change of MP in the presence of various concentrations of EDA. Transmittance spectra for MP@MOPC in air, at the gas chamber and the gas chamber . Performance parameters for previously reported porphyrin based volatile amines sensing systems. Optical shift of the transmittance maximums and minimums of MP@MOPC in the presence of different concentrations of EDA. Estimation of amount of MP inside the PC.

References

[1] L. Spinelle, M. Gerboles, G. Kok, S. Persijn, T. Sauerwald, Review of Portable and Low-Cost Sensors for the Ambient Air Monitoring of Benzene and Other Volatile Organic Compounds, Sensors. 17 (2017) 1520, https://doi.org/10.3390/s17071520.

[2] T.H. Oiamo, M. Johnson, K. Tang, I.N. Luginaah, Assessing traffic and industrial contributions to ambient nitrogen dioxide and volatile organic compounds in a low pollution urban environment, Sci. Total Environ. 529 (2015) 149–157, https://doi.org/10.1016/j.scitotenv.2015.05.032.

[3] W.-H. Chen, Z.-B. Chen, C.-S. Yuan, C.-H. Hung, S.-K. Ning, Investigating the differences between receptor and dispersion modeling for concentration prediction and health risk assessment of volatile organic compounds from petrochemical industrial complexes, J. Environ. Manage. 166 (2016) 440–449, https://doi.org/10.1016/j.jenvman.2015.10.050.

[4] X. Liu, Z. Huang, S. Jia, J. Zhang, K. Li, Y. Luo, The roles of bacteria in the biochemical changes of chill-stored bighead carp (Aristichthys nobilis): proteins degradation, biogenic amines accumulation, volatiles production, and nucleotides catabolism, Food Chem. 255 (2018) 174–181, https://doi.org/10.1016/j.foodchem.2018.02.069.

[5] C. Di Natale, A. Macagnano, E. Martinelli, R. Paolesse, G. D'Arcangelo, C. Roscioni, A. Finazzi-Agrò, A. D'Amico, Lung cancer identification by the analysis of breath by means of an array of non-selective gas sensors, Biosens. Bioelectron. 18 (2003) 1209–1218, https://doi.org/10.1016/S0956-5663(03)00086-1.

[6] N. Zetola, C. Modongo, K. Matlhagela, E. Sepako, O. Matsiri, T. Tamuhla, B. Mbongwe, E. Martinelli, G. Sirugo, R. Paolesse, C. Di Natale, Identification of a Large Pool of Microorganisms with an Array of Porphyrin Based Gas Sensors, Sensors 16 (2016) 466, https://doi.org/10.3390/s16040466.

[7] Y. Hu, X. Ma, Y. Zhang, Y. Che, J. Zhao, Detection of amines with fluorescent nanotubes: applications in the assessment of meat spoilage, ACS Sens. 1 (2016) 22–25, https://doi.org/10.1021/acssensors.5b00040.

[8] L.-Y. Chang, M.-Y. Chuang, H.-W. Zan, H.-F. Meng, C.-J. Lu, P.-H. Yeh, J.-N. Chen, One-minute fish freshness evaluation by testing the volatile amine gas with an ultrasensitive porous-electrode-Capped organic gas sensor system, ACS Sens. 2 (2017) 531–539, https://doi.org/10.1021/acssensors.6b00829.

[9] L. Gil-Sánchez, R. Martínez-Máñez, J.M. Barat, E. Garcia-Breijo, Meat and Fish spoilage measured by electronic tongues, Electron. Noses Tongues Food Sci. Elsevier, 2016, pp. 199–207, https://doi.org/10.1016/B978-0-12-800243-8.00020-2.

[10] S. Wang, J. Liu, H. Zhao, Z. Guo, H. Xing, Y. Gao, Electrically conductive coordination polymer for highly selective chemiresistive sensing of volatile amines, Inorg. Chem. 57 (2018) 541–544, https://doi.org/10.1021/acs.inorgchem.7b02464.

[11] C. Paoletti, M. He, P. Salvo, B. Melai, N. Calisi, M. Mannini, B. Cortigiani, F.G. Bellagambi, T.M. Swager, F. Di Francesco, A. Pucci, Room temperature amine sensors enabled by sidewall functionalization of single-walled carbon nanotubes, RSC Adv. 8 (2018) 5578–5585, https://doi.org/10.1039/C7RA13304A.

[12] R. Thea, D. Onna, M.P. Kreuzer, M. Hamer, Label-free nanostructured sensor for the simple determination of glycosylated hemoglobin (HbA1c), Sensors Actuators B Chem. 297 (2019) 126722, , https://doi.org/10.1016/j.snb.2019.126722.

[13] J.R. Askim, M. Mahmoudi, K.S. Suslick, Optical sensor arrays for chemical sensing: the optoelectronic nose, Chem. Soc. Rev. 42 (2013) 8649, https://doi.org/10.1039/c3cs60179j.

[14] M.A. Martí, S.E. Bari, D.A. Estrin, F. Doctorovich, Discrimination of Nitroxyl and nitric oxide by water-soluble Mn(III) porphyrins, J. Am. Chem. Soc. 127 (2005) 4680–4684, https://doi.org/10.1021/ja044632n.

[15] J. Roales, J.M. Pedrosa, M.G. Guillén, T. Lopes-Costa, S.M.A. Pinto, M.J.F. Calvete, M.M. Pereira, Optical detection of amine vapors using ZnTriad porphyrin thin films, Sensors Actuators B Chem. 210 (2015) 28–35, https://doi.org/10.1016/j.snb.2014.12.080.

[16] R. Rella, J. Spadavecchia, G. Ciccarella, P. Siciliano, G. Vasapollo, L. Valli, Optochemical vapour detection using spin coated thin films of metal substituted phthalocyanines, Sensors Actuators B Chem. 89 (2003) 86–91, https://doi.org/10.1016/S0925-4005(02)00447-1.

[17] S.-K. Lee, I. Okura, Photostable optical oxygen sensing material: platinum tetrakis (pentafluorophenyl)porphyrin immobilized in polystyrene, Int. J. Digit. Analog. Commun. Syst. 34 (1997) 185–188, https://doi.org/10.1039/a701130j.

[18] J. Spadavecchia, G. Ciccarella, P. Siciliano, S. Capone, R. Rella, Spin-coated thin films of metal porphyrin–phthalocyanine blend for an optochemical sensor of alcohol vapours, Sensors Actuators B Chem. 100 (2004) 88–93, https://doi.org/10.1016/j.snb.2003.12.027.

[19] Y. Ding, W.-H. Zhu, Y. Xie, Development of ion chemosensors based on porphyrin analogues, Chem. Rev. 117 (2017) 2203–2256, https://doi.org/10.1021/acs.chemrev.6b00021.

[20] K. Deasy, K.N. Sediq, S. Brittle, T. Wang, F. Davis, T.H. Richardson, D.G. Lidzey, A chemical sensor based on a photonic-crystal L3 nanocavity defined in a silicon-nitride membrane, J. Mater. Chem. C Mater. Opt. Electron. Devices 2 (2014) 8700–8706, https://doi.org/10.1039/C4TC01320D.

[21] H. Inan, M. Poyraz, F. Inci, M.A. Lifson, M. Baday, B.T. Cunningham, U. Demirci, Photonic crystals: emerging biosensors and their promise for point-of-care applications, Chem. Soc. Rev. 46 (2017) 366–388, https://doi.org/10.1039/

C6CS00206D.
[22] M. Scalora, M.J. Bloemer, A.S. Pethel, J.P. Dowling, C.M. Bowden, A.S. Manka, Transparent, metallo-dielectric, one-dimensional, photonic band-gap structures, J. Appl. Phys. 83 (1998) 2377–2383, https://doi.org/10.1063/1.366996.
[23] R.V. Nair, R. Vijaya, Photonic crystal sensors: an overview, Prog. Quantum Electron. 34 (2010) 89–134, https://doi.org/10.1016/j.pquantelec.2010.01.001.
[24] M.C. Fuertes, F.J. López-Alcaraz, M.C. Marchi, H.E. Troiani, V. Luca, H. Míguez, G.J.A.A. Soler-Illia, Photonic crystals from ordered mesoporous thin-film functional building blocks, Adv. Funct. Mater. 17 (2007) 1247–1254, https://doi.org/10.1002/adfm.200601190.
[25] L.D. Bonifacio, B.V. Lotsch, D.P. Puzzo, F. Scotognella, G.A. Ozin, Stacking the nanochemistry deck: structural and compositional diversity in one-dimensional photonic crystals, Adv. Mater. 21 (2009) 1641–1646, https://doi.org/10.1002/adma.200802348.
[26] M.C. Fuertes, S. Colodrero, G. Lozano, A.R. González-Elipe, D. Grosso, C. Boissière, C. Sánchez, G.J. de A.A. Soler-Illia, H. Míguez, Sorption properties of mesoporous multilayer thin films, J. Phys. Chem. C 112 (2008) 3157–3163, https://doi.org/10.1021/jp710612y.
[27] N. Hidalgo, M.E. Calvo, M.G. Bellino, G.J.A.A. Soler-Illia, H. Míguez, Porous supramolecularly templated optical resonators built in 1D photonic crystals, Adv. Funct. Mater. 21 (2011) 2534–2540, https://doi.org/10.1002/adfm.201002486.
[28] M. Hamer, R.M. Caraballo, P.J. Eaton, C. Medforth, Nanoparticles as template for porphyrin nanostructure growth, J. Porphyr. Phthalocyanines 23 (2019) 526–533, https://doi.org/10.1142/S1088424619500469.
[29] S. Colodrero, M. Ocaña, H. Míguez, Nanoparticle-based one-dimensional photonic crystals, Langmuir 24 (2008) 4430–4434, https://doi.org/10.1021/la703987r.
[30] L. González-García, G. Lozano, A. Barranco, H. Míguez, A.R. González-Elipe, TiO2–SiO2 one-dimensional photonic crystals of controlled porosity by glancing angle physical vapour deposition, J. Mater. Chem. 20 (2010) 6408, https://doi.org/10.1039/c0jm00680g.
[31] M.E. Calvo, O. Sánchez-Sobrado, S. Colodrero, H. Míguez, Control over the structural and optical features of nanoparticle-based one-dimensional photonic crystals, Langmuir 25 (2009) 2443–2448, https://doi.org/10.1021/la8030057.
[32] I. Pavlichenko, A.T. Exner, M. Guehl, P. Lugli, G. Scarpa, B.V. Lotsch, Humidity-enhanced thermally tunable TiO 2 /SiO 2 bragg stacks, J. Phys. Chem. C. 116 (2012) 298–305, https://doi.org/10.1021/jp208733t.
[33] D. Onna, K.M. Fuentes, C. Spedalieri, M. Perullini, M.C. Marchi, F. Alvarez, R.J. Candal, S.A. Bilmes, Wettability, Photoactivity, and Antimicrobial Activity of Glazed Ceramic Tiles Coated with Titania Films Containing Tungsten, ACS Omega 3 (2018) 17629–17636, https://doi.org/10.1021/acsomega.8b03339.
[34] M. Kosmulski, Chemical Properties of Material Surfaces, 1st editio, CRC Press, Boca Raton, 2001, https://doi.org/10.1201/9780367800482.
[35] J. Mack, M.J. Stillman, Electronic structures of metal phthalocyanine and porphyrin complexes from analysis of the UV–Visible absorption and magnetic circular dichroism spectra and molecular orbital calculations, Porphyr. Handb. Elsevier, 2003, pp. 43–116, https://doi.org/10.1016/B978-0-08-092390-1.50008-4.
[36] J.F. Angiolini, M. Stortz, P.Y. Steinberg, E. Mocskos, L. Bruno, G. Soler-Illia, P.C. Angelomé, A. Wolosiuk, V. Levi, Diffusion of single dye molecules in hydrated TiO 2 mesoporous films, Phys. Chem. Chem. Phys. 19 (2017) 26540–26544, https://doi.org/10.1039/C7CP05186G.
[37] P.C. Angelomé, M.C. Fuertes, G.J.A.A. Soler-Illia, Multifunctional, Multilayer, Multiscale: Integrative Synthesis of Complex Macroporous and Mesoporous Thin Films with Spatial Separation of Porosity and Function, Adv. Mater. 18 (2006) 2397–2402, https://doi.org/10.1002/adma.200600439.
[38] Theorethical, electrontransferand physical studies. in: K.M. Kadish, R. Guilard, K.M. Smith (Eds.), Handb. Porphyr. Sci. With Appl. to Chem. Physics, Mater. Sci. Eng. Biol. Med. vol. 14, World Scientific Pub Co Inc, 2010, pp. 380–385.
[39] M. Hamer, J.P. Tomba, I.N. Rezzano, Optical properties and sensor applications of bimetallic nanostructures of porphyrins, Sensors Actuators B Chem. 193 (2014) 121–127, https://doi.org/10.1016/j.snb.2013.11.077.
[40] M. Hamer, R.R. Carballo, I.N. Rezzano, Enzyme mimic of heterobimetallic Cu(II) and Fe(III) tetrapyridylporphine modified nanoparticles, Sensors Actuators, B Chem. 160 (2011), https://doi.org/10.1016/j.snb.2011.09.063.
[41] H.A. Benesi, J.H. Hildebrand, A spectrophotometric investigation of the interaction of iodine with aromatic hydrocarbons, J. Am. Chem. Soc. 71 (1949) 2703–2707, https://doi.org/10.1021/ja01176a030.
[42] M. Rahman, H.J. Harmon, Absorbance change and static quenching of fluorescence of meso-tetra(4-sulfonatophenyl)porphyrin (TPPS) by trinitrotoluene (TNT), Spectrochim. Acta Part A Mol. Biomol. Spectrosc. 65 (2006) 901–906, https://doi.org/10.1016/j.saa.2006.01.029.
[43] P. Ganter, B.V. Lotsch, Photonic nanoarchitectonics with stimuli-responsive 2D materials, Mol. Syst. Des. Eng. (2019), https://doi.org/10.1039/C8ME00112J.
[44] B.V. Lotsch, G.A. Ozin, Clay bragg stack optical sensors, Adv. Mater. 20 (2008) 4079–4084, https://doi.org/10.1002/adma.200800914.

Rolando Caraballo PhD in Chemistry from the University of Buenos Aires. His thesis involved the study of photoactivatable ruthenium complexes for materials functionalization. He works at INS under the direction of Galo Soler Illia and Mariana Hamer, using porphyrins for nanomaterials development with applications in renewable energies and sensing.

Diego Onna Has a Chemistry degree and a PhD from the University of Buenos Aires. He is part of Dr. Galo Soler Illia's group and currently working on the combination of rational design of nanostructured materials with multidimensional analysis of signals for the development of modular platforms for the colorimetric detection of analytes with biological relevance.

Nicolás López Abdala Materials Engineer from the University of San Martín and graduated from the National College of Buenos Aires. He entered the Institute of Nanosystems to carry out his doctoral thesis under the direction of Dr. Galo Soler Illia. He is developing a research entitled Vapor Sensors based on functionalized thin mesoporous films: Towards the development of photonic noses.

Galo Soler Illia, Principal researcher CONICET, Studied Chemistry (MSc and PhD) at Buenos Aires University, and completed a postdoc at University Pierre-et-Marie-Curie, Paris. He worked as a CONICET researcher at the Argentine Atomic Energy Commission for more than 10 years. He has published more than 145 papers in reviewed journals, which received more than 10.000 citations (h = 46), and filed four patents. He has published science dissemination books about chemistry and nanotechnology, and leads national and international projects with research groups and companies. He designs and produces new nanosystems with intelligent architectures and custom properties using chemical methods inspired by Nature, with applications in chemical reactors, sensors, and optics.

Mariana Hamer Associate researcher CONICET, PhD in Pharmacy and Biochemistry from the University of Buenos Aires (UBA) She is specialized in the design and development of electrochemical and optical nanoparticulated porphyrinic sensors. She published 13 articles in international scientific journals, exhibited in more than 25 congresses and participates in a PICT-Start Up project. She received the Ducloux Award (2015) from the Argentinian Chemical Association, the UBA Academic Excellence Award (2016 and 2017) and the INNOVAR Award (2016) in the category New Technologies in Scientific Research.